Utilization of a Protein "Shuttle" To Load Vault Nanocapsules with Gold Probes and Proteins

Lisa E. Goldsmith,[†] Melody Pupols,[‡] Valerie A. Kickhoefer,[‡] Leonard H. Rome,[‡,§] and Harold G. Monbouquette[†,§,*]

[†]Chemical and Biomolecular Engineering Department, [‡]Department of Biological Chemistry, David Geffen School of Medicine at UCLA, and [§]California NanoSystems Institute, University of California, Los Angeles, California 90095

ABSTRACT Vaults are large protein nanocapsules that may be useful as drug delivery vehicles due to their normal presence in humans, their large interior volume, their simple structural composition consisting of multiple copies of one protein, and a recombinant production system that also provides a means to tailor their structure. However, for vaults to be effective in such applications, efficient means to load the interiors of the capsules must be demonstrated. Here we describe the use of a domain derived from a vault lumen-associated protein as a carrier to target both gold nanoclusters and heterologous His-tagged proteins to specific binding sites on the vault interior wall.

KEYWORDS: vaults · protein shuttle · nanoencapsulation · drug delivery vehicle · gold clusters

Many common chemotherapeutic agents are small hydrophobic molecules with limited aqueous solubility that require the use of potentially toxic organic solvents for effective delivery.[1] Encapsulating such drugs within hydrophilic carriers may improve drug stability, solubility, and pharmacokinetic properties,[2] in addition to aiding in targeted delivery of the drugs to their desired locations. Similar benefits of encapsulation are expected for protein and peptide-based anticancer agents.[3] Carriers in the size range of 10−100 nm may penetrate solid tumors with high specificity[4] *via* the enhanced permeability and retention (EPR) effect. Common nanoscale drug/gene delivery systems include viral capsids (30−100 nm), liposomes (30−200 nm), and polymer particles (50−2000 nm).[2] Although viruses have proven useful as vaccines,[5,6] their well-documented immunogenicity can produce life-threatening immune responses when used as gene or drug delivery vehicles.[7] During circulation, liposomes commonly exhibit low physical and chemical stability.[8,9] PEGylation of liposomes has been shown to increase their antitumor efficacy but has the side effect of increased skin toxicity.[9] Block copolymer micelles also exhibit physical instability and disassemble if they are diluted below their critical micelle concentration during injection.[10,11] An ideal drug delivery vehicle should be biocompatible and capable of protecting the encapsulated drug from premature degradation, releasing its contents only upon reaching the target tissues.[2,4]

Vaults,[12,13] large (13 MDa) ribonucleoprotein capsules (72.5 × 41 nm) with an interior cavity (5 × 10^7 Å^3) large enough to encapsulate hundreds of proteins, constitute a new, potentially attractive drug delivery vehicle. Vaults are ubiquitous intracellular components of most eukaryotes, including humans, at 10^4−10^5 particles per cell,[14] giving them the potential to be used as biocompatible nanocapsules. The biological function of native vault particles is unknown; however, they have been implicated in numerous pathways including multidrug resistance,[15−17] signal transduction,[18] and nucleocytoplasmic transport, suggesting that vaults may naturally function as carriers. Recently, a role for vaults was implicated in the innate immune response to bacterial pathogens.[19]

Each native vault is composed of multiple copies of three proteins: 78−96 copies of the 96 kDa major vault protein (MVP),[20,21] which makes up 75% of the vault mass, the 193 kDa vault poly(ADP-ribose) polymerase (VPARP), the 290 kDa telomerase associated protein 1 (TEP1), and an untranslated RNA.[12,22] The vault RNA and the two minor proteins, VPARP and TEP1, are found in native vaults at ~6, 8, and 2 copies per vault, respectively.[23] These minor components, however, are not required for capsule formation.[12,24] CryoEM analysis has revealed that the vault has a smooth

*Address correspondence to hmonbouq@ucla.edu.

Received for review May 28, 2009 and accepted September 17, 2009.

Published online September 23, 2009.
10.1021/nn900555d CCC: $40.75

exterior surface with most of the protein present in a thin shell surrounding a large internal cavity.[12,22]

Expression of a cDNA encoding MVP in insect cells results in the production of self-assembled vault particles.[24] Recombinant vaults have biochemical characteristics and structures virtually indistinguishable from native rat vaults[12] and are taken up by HeLa cells *in vitro*,[25] possibly through endosomal pathways. Along with their expected biocompatibility, vaults possess several features that make them well-suited as drug delivery vehicles including their self-assembled capsular-like structure, large lumen, and recombinant expression system that allows for the ability to produce large quantities of specifically designed vaults. CryoEM analysis of various recombinant vaults revealed the location of the N-termini and C-termini to be inside the vault at the waist and outside at the particle caps, respectively.[12,20] Recently, a 3.5 Å resolution crystal structure was published that confirmed the cryoEM locations of the N- and C-termini.[21] In this study, we use CP-MVP-VSVG recombinant vaults that contain a cysteine-rich 12 amino acid peptide tag (CP) appended to the N-terminus of MVP, as well as an 11 amino acid tag derived from vesicular stomatitis virus glycoprotein (VSVG) fused to the MVP C-terminus. The ability to generate vaults with external peptide tags is useful for targeting vaults to specific locations.[26]

When deposited on positive surfaces and imaged using freeze etch EM with platinum shadowing, native vaults disassemble at their waist, and each half vault further opens into a flower-like structure.[22] Using a combination of techniques, including intrinsic fluorescence, fluorescence quenching, light scattering, quartz crystal microbalance surface adsorption, and negative-stain TEM, we showed that similar disassembly of recombinant vaults could be triggered by lowering solution pH to <4.0,[27] suggesting that conditions inside lysosomal compartments might trigger vault opening. In addition to this triggered disassembly, vaults undergo transient opening in solution, allowing encapsulation of large vault-associated proteins, TEP1 and VPARP,[28] as well as semiconducting polymers,[29] within preformed vaults. Proposed modes of vault dynamics *in vivo* include transient splitting at the vault waist, flipping open of individual MVP subunits or groups of subunits, or a combination of both.[28] Recently, it was shown that transient vault opening could be limited by joining the vaults' halves using a pH-labile cross-linker.[30] Control of such conformational changes will be useful in our efforts to load desired materials into the vault lumen.

The mINT protein (22.7 kDa) is the minimal interaction domain (162 amino acids) derived from the C-terminus of VPARP that binds to MVP on the vault inner surface. The mINT is known to enter the vault through transient vault openings and interacts specifically with the N-terminal half of the vault MVP sequence.[12,25,31,32] When heterologous proteins such as luciferase or green fluorescent protein (GFP) are fused to mINT, these proteins can be sequestered inside vaults. Indeed, the vault interior serves as a protective environment for the encapsulated proteins, which retain their native enzymatic and fluorescent properties.[25]

By exploiting mINT's ability to enter and "dock" within the vault lumen, one aim of this study is to utilize mINT to sequester compounds within vaults that are not encoded in DNA, the common situation with small molecule drugs. Purified recombinant mINT contains an additional 31 amino acids at the N-terminus that includes a 6-His tag, a thrombin cleavage site, and a T7 tag. To demonstrate initially the use of the mINT domain to shuttle bound species into vaults, we utilized Ni−NTA−nanogold, a material with affinity to the 6-His tag at the N-terminus of mINT, as a model cargo. The gold can be identified easily by TEM. A specific interaction of the gold clusters with 6-His-tagged recombinant mINT is demonstrated, as well as the ability of mINT to shuttle gold probes inside the vaults and bind to the vault interior. With the ultimate goal of developing vaults for use as a drug delivery system, the studies outlined here with Ni−NTA−gold clusters serve to establish the mINT protein as a "shuttle" that is able to target desired chemical species to the vault interior.

Further, use of the gold−mINT complex described above may be extended to serve as a platform for encapsulating any desired His-tagged peptide or protein. Association of a His-tagged protein or peptide with the gold−mINT complex may be achieved by simple mixing, eliminating the need to re-engineer the mINT protein itself. In this work, linkage of 6-His-tagged GFP to the gold−mINT complex and its transport to the vault interior demonstrates a potentially versatile method for loading His-tagged protein or peptide therapeutics in vaults without the need to fuse the desired protein to mINT directly.

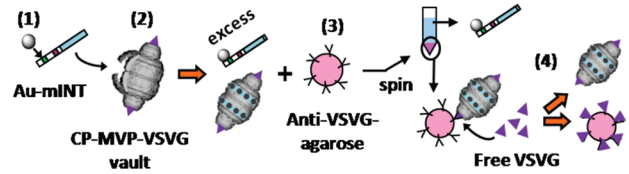

Figure 1. Schematic diagram of the formation and purification of the gold−mINT/vault complexes. (1) Gold (Au) binds to the 6-His residues on the N-terminus of purified mINT to form Au−mINT. (2) Au−mINT enters the vault through transient vault openings and associates with the vault interior. (3) CP-MVP-VSVG vaults (see Methods) and their encapsulated contents (Au−mINT) are separated from excess free species through binding of the C-terminal VSVG peptide with anti-VSVG-agarose. (4) Following centrifugation, the pellet (and supernatant) fractions can be analyzed by parallel Western blot and silver development to detect successful complex encapsulation. Alternatively, addition of free VSVG peptide releases loaded vaults from beads, which may then be visualized by TEM or used in fluorescence quenching studies.

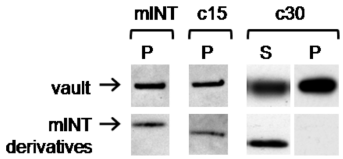

Figure 2. C-terminal truncations of mINT to reduce the vault interaction domain. Western blot analyses of mINT, c15 (mINT shortened by 15 amino acids), and c30 (mINT shortened by 30 amino acids) encapsulated within CP-MVP-VSVG vaults and pulled down using anti-VSVG sepharose beads (P lanes). The upper row of blots resulted from probing with an anti-VSVG antibody for vaults, whereas the lower row arose from use of an anti-VPARP antibody for mINT derivatives. While mINT and c15 co-immunoprecipitated with vaults, c30 remained entirely in the supernatant (S lane) and was not pulled down with vaults.

RESULTS AND DISCUSSION

This work entailed the encapsulation of noncovalently bound species within vaults utilizing the "full-length" 162 amino acid mINT protein as a shuttle, unless otherwise indicated. The general approach taken is illustrated in Figure 1. In summary, a functionalized gold nanoparticle, here representing a small molecule drug or imaging agent, was bound to the 6-His tag of the mINT protein, forming a gold−mINT (Au−mINT) complex. Through opening of vault subunits,[28] the gold−mINT complex entered the vault particle, bound to the inside compartment, and remained associated following further purification. In addition to encapsulation of the gold−mINT complex, any desired peptide or protein therapeutic could be encapsulated using this strategy provided it has a His-rich tag. In this study, this latter approach is demonstrated using 6-His-tagged GFP.

Vault Binding by mINT and Truncated mINT Proteins. The ability of the mINT domain to target fused proteins to the inside of vaults and provide a protective environment was demonstrated previously.[25,28] To determine whether the 162 amino acids of mINT could be further reduced and yet retain its ability to bind to vaults, selective deletions of 15 amino acids (an arbitrarily chosen length) from the C-terminus were made. The molecular weights of the c15 and c30 proteins were calculated based on the amino acid sequence to be 21.1 and 19.4 kDa, respectively. The association of mINT and its truncated derivatives with vaults was tested by immunoprecipitation. A previous study showed that the C-terminal VSVG epitope tag on recombinant vaults is accessible to antibody binding.[26] Therefore, the association of mINT and its truncated derivatives with VSVG-tagged recombinant vaults was tested by immunoprecipitation with anti-VSVG antibody immobilized on Protein G sepharose beads. The results are shown in Figure 2. Excesses of all three mINT constructs remained in the supernatant (similar to the supernatant of the c30-containing sample, as depicted) and could be detected by the anti-mINT antibody. mINT (amino acids 1563−1724 of VPARP) and c15 (amino acids 1563−1709) both were encapsulated and pulled down with the beads (P lanes) indicative of binding to vaults. However, c30 (amino acids 1563−1694) remained entirely in the supernatant and was not observed in the pellet fraction with vaults. Thus, c30, an abbreviated version of mINT which does not bind to the vault interior, is used here as a negative control for mINT encapsulation.

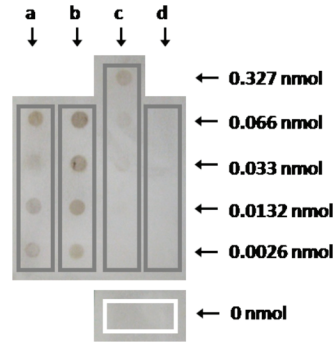

Figure 3. Detection of gold binding to His-tagged proteins. 6-His-tagged (a) mINT, (b) c30, and (c) GFP-INT as well as (d) BSA or buffer (white box, 0 nmol protein) were spotted onto a nitrocellulose membrane. After blocking with 5% BSA, and incubating in 1:50 dilution of Ni−NTA−gold clusters in 1% BSA, the membrane was developed using LI silver to detect gold attachment.

6-His Tag of mINT Facilitates Association of Ni−NTA−Gold Clusters with Vaults. The mINT and its derivatives have been engineered with an N-terminal 6-His tag for ease of purification; however, these tags were utilized here as the attachment points for a functionalized gold nanocluster. As proof of concept, 1.8 nm Ni−NTA−nanogold gold clusters[33] (~15 kDa) were attached to the 6-His tag of the mINT protein,[34] forming a Au−mINT complex. Attachment of Ni−NTA−gold clusters to the 6-His-tagged proteins used in this study was confirmed by dot blot analysis. Figure 3 shows that all three 6-His-tagged proteins, mINT (a), c30 (b), and GFP-INT (c), were able to interact with Ni−NTA−gold clusters, while BSA (d), which lacks a 6-His tag, and buffer only (white box in Figure 3) did not. On the basis of a comparison of equal amounts of His-tagged protein (across each row), it appears that interaction of Ni−NTA−gold clusters with the 6-His tag is more favorable (darker signal) for the smallest protein c30 (~19 kDa) and is less favorable for the larger GFP-INT (~55 kDa); perhaps indicating a greater accessibility of the 6-His tag on the smaller protein. This difference may also be due to an increase in the number of the smaller c30 molecules bound to the membrane, as compared to the larger GFP-INT. Regardless, Ni−NTA−gold clusters bound to all of the 6-His constructs tested.

The specific association of the Ni−NTA gold clusters with vault MVP *via* the 6-His tag of mINT was demonstrated using the Au−mINT complexes described above. The mINT and Au−mINT were incubated with vaults and pulled down by immunoprecipitation with anti-VSVG agarose beads (P lanes) (Figure 4). Thrombin pretreatment of the mINT protein cleaved off the 6-His tag fragment, resulting in a loss of ~2 kDa (lane 5). As

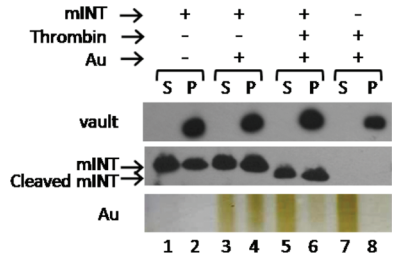

Figure 4. The 6-His tag of mINT facilitates association of gold clusters with vaults. Parallel Western blot and LI silver-enhanced SDS−PAGE analyses of gold (bottom panel) associated with CP-MVP-VSVG vaults (top) through interaction with mINT (middle). Vaults were separated from excess free species in the supernatant (S lanes) by pull-down using anti-VSVG-agarose (P lanes), which recognizes VSVG peptides displayed on the outside of the vault.[26] Gold nanoparticles associated with the vault only when mINT was used as a mediator (lane 4 *vs* lane 8). However, thrombin pretreatment of the mINT protein cleaved the 6-His tag from mINT, and Ni−NTA−gold clusters coordinated to the 6-His tag were no longer pulled down with vaults (lane 6 *vs* lane 4). The upper blot panel was probed with an anti-VSVG antibody for vaults, the middle blot with an anti-VPARP antibody for mINT, and the gel of the bottom panel was enhanced with LI silver to detect the presence of gold. Lanes are labeled along the bottom, as referenced in the text.

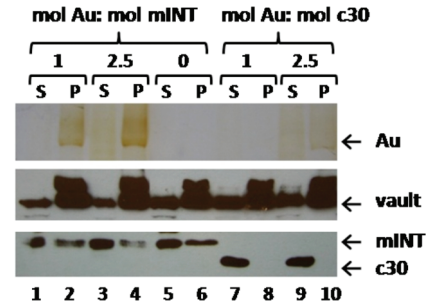

Figure 5. Ability of mINT to bind to the vault interior is necessary for the encapsulation of gold clusters. Parallel Western blot and LI silver-enhanced SDS−PAGE analyses of Ni−NTA−gold clusters (top panel) and mINT or c30 (mINT shortened by 30 amino acids) (bottom) that associated with CP-MVP-VSVG vaults (middle) and were pulled down by anti-VSVG-agarose beads (P lanes). Although the gold clusters bound to c30 (Figure 3), they were not pulled down with vaults (lanes 8 and 10) because c30 cannot bind to the vault interior. Conversely, this suggests that "full-length" mINT, which is known to bind to the vault interior, was required to target gold clusters within vaults (lanes 2 and 4). The gel of the top panel was enhanced with LI silver to detect the presence of gold, and the middle and bottom blots were probed with an anti-VSVG antibody for vaults, and an anti-VPARP antibody for mINT and c30, respectively. Lanes are labeled along the bottom, as referenced in the text.

shown in lane 6, cleaved mINT still associated with the vaults and was pulled down with vaults attached to beads; the gold clusters, however, were no longer pulled down, indicating that thrombin disrupts the interaction between Ni−NTA−gold clusters and the vault binding domain of mINT. Thus, the presence of the 6-His tag is necessary for specific, mINT-mediated association of Ni−NTA−gold clusters with vaults.

Encapsulation of the Attached Ni−NTA−Gold Cluster Probes Are Due to the Ability of mINT To Associate with the Vault Interior. By comparing gold encapsulation within vaults using mINT and c30 (Figure 5), one can assess whether the ability of mINT to enter and associate with the vault interior is critical for association of foreign materials with vaults. His-tagged protein (0.065 nmol) was incubated with or without an equimolar (or 2.5 times greater) amount of Ni−NTA−gold clusters. Vaults and their associated contents were then separated as described previously (Figure 1). Figure 5 shows that Au−mINT was bound specifically to vaults that were pulled down by the antibody beads (lanes 2 and 4), whereas Au−c30 was not (lanes 8 and 10). Although gold binds well to c30 (Figure 3), the c30 itself is unable to bind to the vault interior, suggesting that mINT, a functional binding protein, is required to target attached gold probes to the vault interior.

Regardless of the amount of gold clusters used, c30 does not facilitate loading of gold into vaults (Figure 5, lane 8). However, as the amount of Ni−NTA−gold clusters is increased to 2.5 times the His-tagged protein (on a molar basis), a small amount of Ni−NTA−gold clusters appear to nonspecifically bind to the vault protein itself and are pulled down (Figure 5, lane 10). Thus, although it appears that more gold is pulled down with vault-associated mINT at higher gold concentrations, some of this signal may be excess gold binding to the vault particle itself. Nevertheless, this experiment showed that the vault binding site of mINT is necessary for appreciable gold cluster loading of vaults mediated by VPARP-based shuttles.

Verification That Au−mINT Is Encapsulated within the Vault Lumen. Vaults loaded with gold *via* a mINT protein shuttle were released from antibody beads and incubated in gold enhancer (GEEM) to enlarge the gold particles to a size where they could be visualized by TEM. Multiple electron-dense spots of ~2−6 nm were observed inside the protein shell of Au−mINT and Au−GFP−INT containing vaults (Figure 6), concentrated near the VPARP binding domain (on the N-terminal half of the vault MVP midway between the vault waist and caps, as indicated by dashed lines) located by cryoEM[12] and in a yeast two-hybrid interaction assay.[32] Vaults incubated with gold only (no mINT) as well as Au−c30 vaults did not harbor electron-dense spots because even though Ni−NTA−gold clusters are able to bind to c30, c30 cannot bind to the vault interior. In addition, it is quite possible that more Ni−NTA−gold clusters associated with mINT are encapsulated within vaults than was observed, owing to the necessity to enhance the 1.8 nm gold particle size. Further, very few electron-dense spots were observed to stick to the exterior of the vault shell, even in these two-dimensional images, supporting the notion that the gold particles were effectively shuttled into the vault lumen by mINT or GFP−INT.

Further evidence that the gold probes were, in fact, packaged within the vault lumen was shown by comparing the fluorescence quenching of GFP−INT and

Au−GFP−INT in vaults by congo red to the quenching of the free GFP complexes (Figure 7c). Similar studies were used previously to confirm GFP−INT fusion protein encapsulation within vaults.[25,28] GFP−INT in PBS was found to have two absorbance maxima at ~278 and 490 nm with a shoulder at ~400 nm (Figure 7a) and a fluorescence emission maximum at 511 nm (Figure 7b). Since illumination at 490 nm might interfere with emission monitored at 511 nm, samples were excited at 468 nm (peak of excitation scan) (Figure 7b). At the concentration used (0.11 μM), congo red did not show any fluorescence at 511 nm when excited at 468 nm, and attenuation due to congo red absorbance at both wavelengths was negligible. As compared to an equal amount of soluble GFP−INT, initial Au−GFP−INT fluorescence was approximately half that of GFP−INT (not shown), perhaps due to quenching[35] by Ni^{2+} ions in the nanogold solution, which coordinate the His-tagged GFP−INT to NTA-functionalized gold probes. Figure 7c shows that soluble GFP−INT and Au−GFP−INT were completely quenched within the 10 s time delay needed for quencher addition and mixing (flat traces). In comparison, quenching of GFP−INT and Au−GFP−INT in vaults exhibited delayed quenching kinetics and were fully quenched only after 115 ± 1 and 86 ± 2 s, respectively. Thus, GFP−INT in vaults with or without attached gold clusters displayed delayed quenching, indicating that the GFP−INT (along with Ni−NTA−gold clusters attached to the protein's 6-His tag) was indeed encapsulated inside vaults and was more protected from the outside solution by the surrounding vault shell.

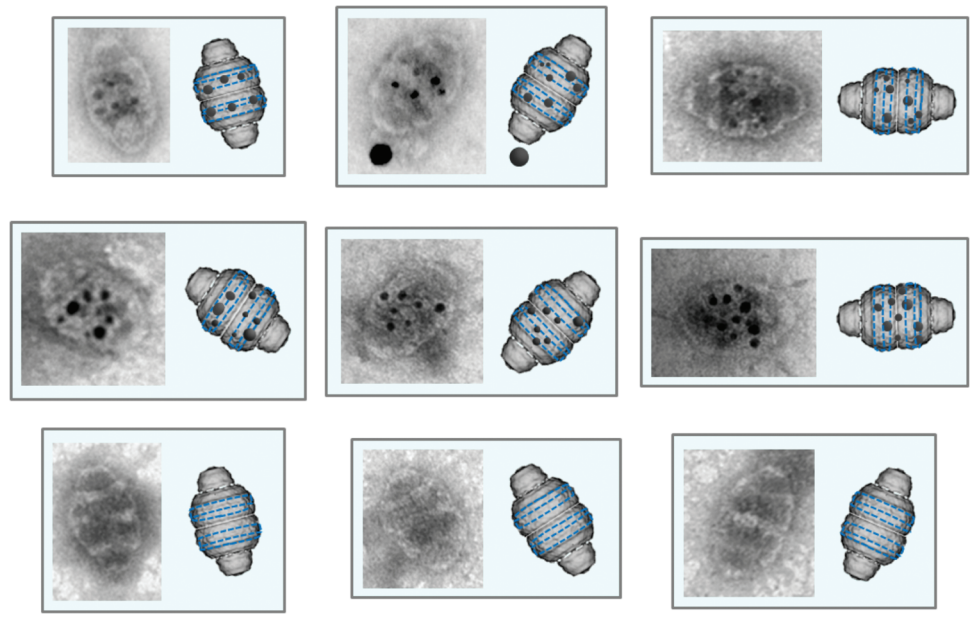

Figure 6. Negative-stain TEM images (left) and corresponding cartoons depicting locales (right) of gold nanoparticles encapsulated within vaults *via* attachment to mINT (top panel) and GFP-INT (middle). After enhancement, Ni−NTA−gold clusters were seen as dark black or gray dots, located near the VPARP binding domain (dashed lines). Vaults incubated with gold attached to c30 (a version of mINT shortened by 30 amino acids) (bottom) did not exhibit electron-dense dot patterns within vaults and appeared empty because c30 is not able to bind to the vault interior (Figure 5). Vaults alone, as well as vaults with mINT, GFP−INT, and c30, but without Ni−NTA−gold clusters, also did not exhibit electron-dense dots within their interiors (not shown). Note that, although the TEM images are two-dimensional cross sections of vaults, we consistently observed gold clusters localized within the interior of the vault outline rather than sticking to the outer edge, indicating targeted encapsulation of the nanoparticles rather than random association with the vault protein.

6-His-GFP Sequestered within Vaults *via* the Au−mINT Shuttle. The studies described above show collectively that NTA-functionalized gold nanoparticles can be attached to the 6-His tag of mINT through Ni^{2+} affinity coordination and shuttled into the vault lumen. Here, the Ni−NTA−gold was used to simultaneously capture the mINT shuttle and another 6-His-tagged protein of interest. As a model protein, we used 6-His-tagged GFP. 6-His-GFP was nonspecifically pulled down with CP-MVP-VSVG vaults by association with the anti-VSVG agarose beads or the vault or mINT proteins unless 0.05% NP40, a nonionic detergent, was present during all incubation and washing steps. Figure 8 shows that, with NP40, 6-His-GFP was only encapsulated within vaults in the presence of both mINT and Au. Encapsulation of 6-His-GFP did not occur without Ni−NTA−gold as a linker to the mINT protein or in the presence of Au but without mINT. Therefore, this approach could serve as a versatile means to sequester within vaults recombinant proteins or peptides with His-rich tags.

By comparing GFP fluorescence of vaults released from beads to positive controls of free His-GFP fluorescence, it was found that the experimental sample (6-His-GFP + Au + mINT encapsulated in vaults) contained ~0.0092 nmol GFP in 95 μL. From Western blot titration, it was determined that the 50 μL of CP-MVP-VSVG s20 used in the preparation of each sample contained ~10 μg (1.0×10^{-3} nmol) vaults. If all of the vaults were released from beads and analyzed by solution fluorescence, this corresponds to ~9 GFP molecules per vault. Although the efficiency of the release of CP-MVP-VSVG vaults from anti-VSVG agarose by addition of VSVG peptide was not quantified, it likely was less than 100%, making the estimate of ~9 GFP molecules per vault a minimum. Thus, using Au as an intermediate to attach a 6-His protein of interest to the mINT shuttle may be a feasible method for loading vaults with protein or peptide therapeutics.

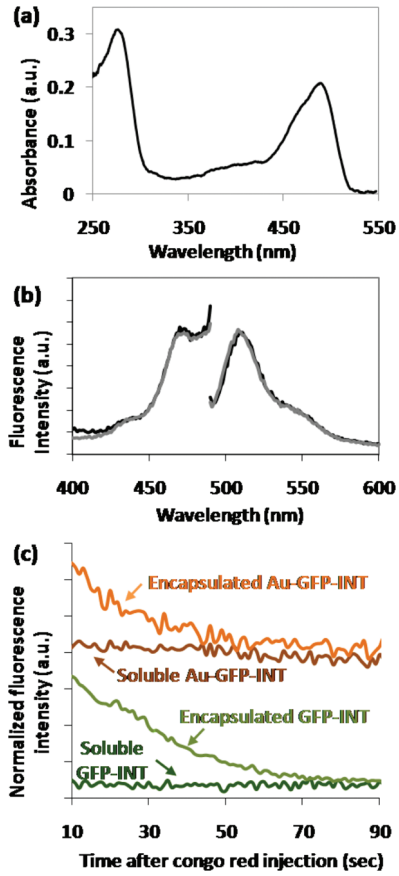

Figure 7. Vault protein shell protects internalized GFP−INT from the outside solution environment. (a) Absorption spectra of 0.24 mg/mL free GFP−INT. (b) Overlapping excitation (left) and emission spectra (right) of soluble GFP−INT (gray traces) and GFP−INT bound in vaults (black traces). Note that the peak excitation was at 468 nm, and the peak emission was at 511 nm. Addition of gold decreased the intensities by approximately half, but did not change the shape of the spectra. (c) Fluorescence quenching of GFP−INT and Au−GFP−INT within vaults by congo red *versus* quenching of the free complexes. Free complexes were quenched within the ~10 s delay needed for quencher addition and mixing (flat traces), while complexes sequestered within vaults exhibited delayed quenching kinetics, indicating that the complexes were indeed encapsulated within the vault lumen.

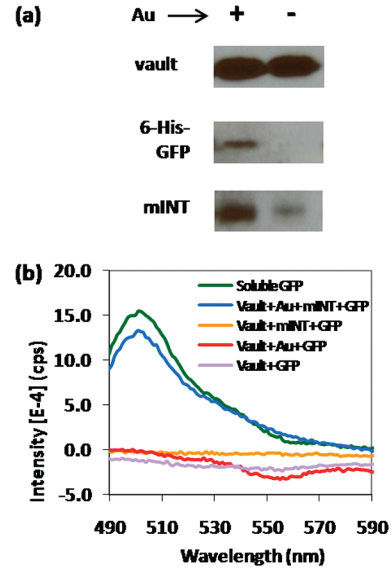

Figure 8. Au−mINT complex can be used as a shuttle to encapsulate within vaults 6-His-tagged GFP. (a) Western blot of 6-His-GFP associated with CP-MVP-VSVG vaults *via* attachment to mINT with or without the gold clusters as an intermediate. Incubation in the presence of 0.05% NP40 resulted in specific entrapment of 6-His-GFP only when it was linked to mINT by gold. The blots were generated by probing preparations with an anti-VSVG antibody for vaults (top panel), an HRP-conjugated anti-His antibody for His-tagged GFP (middle panel), and an anti-VPARP antibody for mINT (bottom panel). (b) GFP emission intensities (excitation wavelength = 468 nm) of samples created in the presence of 0.05% NP40 (see legend). Note that soluble 6-His-GFP alone (3.125 μg/mL) was used as a quantitative positive control.

CONCLUSION

In this work, we illustrate the utility of mINT as a protein shuttle to load vaults with species not fused to the mINT protein itself. We first confirmed using dot blots that Ni−NTA−gold clusters specifically attached to mINT, GFP-INT, and c30 proteins *via* the 6-His tags on the proteins. Immunoprecipitation was used to separate vaults and their encapsulated contents from free complexes in solution. We then demonstrated with parallel Western blot and silver-developed gel electrophoresis analyses that gold clusters were only encapsulated in vaults when preincubated with mINT or GFP−INT. In a parallel analysis, c30 was used as a negative control because, although it can bind Ni−NTA−gold clusters through its 6-His tag, the c30 itself is not able to bind to vaults. Additionally, when thrombin was used to cleave the 6-His tag from mINT, the attached gold clusters were no longer encapsulated within vaults, confirming that the Au−mINT interaction occurs specifically *via* the protein's 6-His tag, enabling binding of the mINT to vaults with minimal interference from the attached moiety. Encapsulation of complexed gold clusters within vaults was confirmed by fluorescence quenching studies of soluble *versus* encapsulated GFP−INT and Au−GFP−INT. Negative-stain TEM after gold enhancement offered visual confirmation. Finally, use of the Au−INT complex to sequester a 6-His-tagged protein (6-His-GFP) within vaults was demonstrated using Western blot and solution fluorescence.

Future studies may examine release of gold probes from loaded vaults. Possible mechanisms of release to be investigated include exposure to low pH (as found in the endosomes and lysosomes), which will simultaneously disassemble the vaults[27] and disrupt the interaction between the Ni−NTA−gold clusters and mINT's 6-His tag (at pH <5).[34,36] Also, appropriate engineering of mINT's cleavage site may enable release *in vivo* of Ni−NTA−gold clusters by cell-specific proteases.

METHODS

Materials. Ni−NTA−nanogold, gold enhancer (GEEM, electron microscopy formulation), and silver enhancer (LI silver) were purchased from Nanoprobes (Yaphank, NY). Monoclonal anti-VSVG antibody produced in mouse, anti-VSVG-agarose antibody (beads) produced in mouse, VSVG peptide, normal goat serum (NGS), normal sheep serum (NSS), congo red, and uranyl acetate dehydrate were obtained from Sigma. ECL Western blotting substrate and Protein G sepharose was purchased from GE Healthcare. Goat anti-rabbit IgG-HRP and BSA were purchased from Biorad. Sheep anti-mouse IgG-HRP was obtained from Amerhsam. Anti-His-HRP (kit #34460) was purchased from Qiagen (Valencia, CA), and 6-His-tagged green fluorescent protein (6-His-GFP) was obtained from Millipore (St. Louis, MO). Thrombin (biotinylated) was obtained from EMD chemicals (Gibbstown, NJ). The anti-MVP and VPARP polyclonal rabbit antibodies have been described previously.[16,31] All buffer components were of analytical grade or better.

Preparation of Recombinant Proteins. CP-MVP-VSVG recombinant vaults contain a cysteine-rich 12 amino acid peptide tag (CP) appended to the N-terminus of MVP, as well as an 11 amino acid tag derived from vesicular stomatitis virus glycoprotein (VSVG) fused to the MVP C-terminus. The C-terminal VSVG tags are localized on the outside of the particle[26] and are used here to rapidly purify vault particles from crude extracts. CP-MVP-VSVG infected Sf9 cells were prepared as described.[12,24] Cells were spun for 5 min at 437.5*g*, and the cell pellet was washed in Dulbecco's PBS (pH 7.2) and stored at −80 °C as 0.05 g of wet cell pellet aliquots. Immediately before use, an aliquot was thawed on ice, lysed in 247.5 μL buffer A (50 mM Tris-HCl, pH 7.4 + 75 mM NaCl + 0.5 mM $MgCl_2 \cdot 6H_2O$) + 1% Triton X-100 + 2.5 μL EDTA-free protease inhibitor (PI) cocktail (Sigma). After spinning at 18 000*g* for 20 min at 4 °C, the supernatant containing vaults (s20 crude extract) was recovered. Vaults were further purified, along with encapsulated contents, using immunoprecipitation with anti-VSVG-agarose as detailed below. The concentration of vaults in extracts was determined by Western blot titration against known quantities of CP-MVP vaults that had been purified by sucrose gradient centrifugation[24] and quantified with a BCA protein assay (Pierce). The Western blot membrane was probed with anti-MVP and goat anti-rabbit-HRP and developed with ECL reagents. The Western blot film was scanned and intensities of MVP bands were quantified using a densitometer (calibration curve plotted on a semilog scale had a slope of 3680).

The VPARP-based shuttle proteins used in this study were mINT (amino acids 1563−1724 of VPARP) and three derivatives: c15, a C-terminal 15 amino acid deletion of mINT (amino acids 1563−1709), a C-terminal 30 amino acid deletion of mINT (amino acids 1563−1694), and a fluorescent GFP−INT fusion protein (55 kDa).[25] The construction of the mINT− and GFP−INT pET28 expression vectors is described elsewhere.[25,28] The c15 and c30 deletions were amplified by PCR from the mINT cDNA in pET28a(+) (Novagen) using a T7 forward primer and reverse primers (5′-CCCCCTCGAGTTATATGGGCTGGAGTCCCAG-3′ or 5′-CCCCCTCGAGTTAGTTCCCCAGTTCAAGCCGTGGGCA-3′ for c15 or c30, respectively) which include Xho1 sites. The PCR products were digested with EcoR1 and Xho1 and cloned into the corresponding sites in the *Escherichia coli* bacterial expression vector, pET28a(+). The mINT, c15, and c30 proteins were then expressed in the BL21-CodonPlus *E. coli* strain (Stratagene) and released from cells by sonication. GFP−INT protein was released from cells using BugBuster (Novagen). All four proteins were then purified using His-bind metal ion affinity columns (Novagen). Eluted proteins were dialyzed against buffer A containing 10% glycerol, 0.1 mM EDTA, and 1 mM DTT for 1 h and then buffer A + 10% glycerol overnight at 4 °C and stored in frozen aliquots at −80 °C until use. Protein concentrations were determined by the BCA protein assay.

Dot Blot. Ten microliter serial dilutions of purified mINT, c30, and BSA were absorbed onto a presoaked nitrocellulose membrane using a Bio-Dot apparatus (Biorad) and allowed to filter by gravity for 10 min, followed by an additional 5 μL of buffer for 5 min. The apparatus was disassembled, and the membrane was then washed in TBS (50 mM Tris base + 150 mM NaCl) plus 0.5% Tween 20 (TBST), blocked in 5% BSA or milk in TBST for 30 min at room temperature, rinsed, and incubated with a 50× dilution of Ni−NTA−gold clusters + 1% BSA in TBST for 30 min at room temperature. After rinsing thoroughly in TBST and water, the membrane was developed using LI silver for 15 min, washed with water, and exposed to fresh LI silver for another 10 min.

Evaluation of mINT Derivatives for Association with Vaults. The mINT constructs lacking 15 or 30 C-terminal amino acids (c15 and c30, respectively) were evaluated for their potential to associate with vaults. A deletion that no longer associated with vaults would serve as a negative control for mINT binding. Ten microliters of CP-MVP-VSVG vault extract was added to 5 μg of purified c15 or c30 protein, or to 25 μL of crude extract of induced *E. coli* expressing full-length mINT, and the volume was brought up to 200 μL with buffer A + 1 mM DTT + PI. The mixture was incubated for 1 h on ice to allow for association of mINT and derivative constructs with the vault interior. Protein G sepharose was buffer exchanged as per the product protocol into the same buffer. Twenty-five microliters of buffer-exchanged Protein G sepharose and 1 μL of a 1:4 dilution of anti-VSVG antibody were added to each sample, and samples were tumbled at 4 °C for 1 h. CP-MVP-VSVG vaults and their encapsulated contents were separated from free species by spinning down the sepharose at 370*g* for 2 min. The supernatant was collected, and the beads were washed three times with 0.5 mL of buffer A + 1 mM DTT + PI. Loaded vaults were resuspended in 50 μL of SDS sample buffer and were released from beads by denaturation at 100 °C for 5 min. Beads were again spun at 370*g* for 2 min, and the supernatant (containing species previously bound to beads) was fractionated on SDS−PAGE. Association of mINT, c15, and c30 (identified using an anti-mINT antibody) with vaults was then analyzed by Western blot.

Loading and Immunopurification of Vaults Containing Gold and 6-His-Tagged GFP. The procedure for loading vaults with Ni−NTA−gold clusters is depicted in Figure 1. Briefly, 0.065 nmol of mINT (or c30 or GFP-INT) was incubated in 40 μL of pH 7.6 PBS buffer (PBS) with or without Ni−NTA−nanogold for 1 h at room temperature to form a complex (Au−mINT, Au−c30, or Au−GFP−INT). Attachment of 0.065 nmol 6-His-GFP to the Au−mINT complex (GFP−Au−mINT) was performed by simultaneous incubation of mINT, 6-His-GFP, and Au in 60 μL of PBS pH 7.6 containing 0.05% NP40 for 1 h at room temperature. For thrombin cleavage studies, mINT was preincubated in PBS plus 20 mM imidazole (to reduce nonspecific binding of the gold to single His residues on the mINT or vaults) with or without the recommended 0.005 U thrombin/μg His-tagged protein for 1 h at room temperature. For all samples (with or without thrombin), 20 μL of vault extracts containing ∼1 μg of vaults was added to each sample and incubated on ice for 1 h, allowing the Au−mINT complex to enter and associate with the vault interior. Anti-VSVG-agarose (25 μL buffer-exchanged with pH 7.6 PBS) was added to each sample, the volume brought up to 420 μL with PBS pH 7.6 buffer (to keep the beads suspended), and samples were tumbled at 4 °C for 1 h. CP-MVP-VSVG vaults and their encapsulated contents were separated from free species by spinning down the agarose at 370*g* for 1 min and washed three times with PBS. Loaded vaults were denatured by heating at 100 °C for 5 min and released into the supernatant. Beads were again spun at 370*g* for 1 min, and the supernatant (containing species previously bound to beads) was fractionated on SDS−PAGE and then analyzed in parallel by silver staining (with LI silver) or Western blotting. Alternatively, 25 μL of 1 mg/mL of VSVG peptide in PBS was added to samples and incubated for 30 min at room temperature to release loaded vaults from beads. Beads were then pelleted, and the supernatants containing vaults were collected and used for either TEM or fluorescence analyses.

Gel Electrophoresis and Western Blots. Loaded vault samples were prepared as described above using ∼1 μg vaults, 0.065 nmol of 6-His-tagged proteins, and 25 μL of VSVG antibody beads. The amount of Ni−NTA−gold clusters used was equivalent to the amount of 6-His-tagged protein (1:1) or 2.5 times greater (2.5:1 mol Au/mol His-tagged protein), as indicated in the figures. After immunoprecipitation, the samples were spun to separate free gold clusters or mINT in the supernatant (S fractions) from loaded vaults attached to beads (pulled down in the P fraction). Samples were denatured in SDS sample buffer without reducing

agent (as reducing agent may degrade the Ni−NTA−nanogold)[37] and loaded on parallel SDS−PAGE gels. After thoroughly rinsing in water, one gel was developed using two fresh preparations of LI silver to detect the presence of gold. The parallel gel was transferred onto a nitrocellulose membrane, blocked for 30 min in 5% milk in TBST, washed three times in TBST, shaken in primary antibody for 1 h at room temperature (or overnight at 4 °C), washed in TBST, shaken in secondary antibody for 1 h at room temperature, washed in TBST, and developed. Primary antibodies detected the ~100 kDa CP-MVP-VSVG monomer (1:2000 anti-VSVG + 5% normal sheep serum (NSS)) and the interaction domains of mINT and GFP−INT, as well as c30 (1:1000 anti-VPARP + 5% normal goat serum (NGS)). Secondary antibodies used were 1:2000 sheep anti-mouse-HRP + 5% NSS, and 1:2000 goat anti-rabbit-HRP + 5% NGS to detect vault and interaction domains, respectively. To detect 6-His-GFP, the membrane was blocked in the supplied blocking reagent for 1 h at room temperature, washed three times in TBST and twice in TBS, incubated in anti-His-HRP diluted 1:1000 in blocking reagent for 2 h at room temperature, washed twice in TBST and twice in TBS, and developed.

TEM. Au−mINT, Au−GFP−INT, or Au−c30 vaults were prepared and purified as described above. Loaded vaults were released from beads by incubation with 25 μL of 1 mg/mL of VSVG peptide in PBS for 30 min at room temperature. Beads were then pelleted (370*g*, 1 min), and detached vaults were recovered in the supernatant. Ten microliters of released vaults was preincubated with 15 μL of fresh gold enhancer (GEEM) for 5 min to enhance the 1.8 nm nanogold so it could be visualized using the JEM 1200-EX transmission electron microscope (JEOL, Tokyo, Japan). Samples were then absorbed on nanoporous carbon-coated copper grids for 5 min and stained with 1% uranyl acetate in water for 5 min to visualize the vaults themselves.

Fluorescence and Fluorescence Quenching. GFP−INT vaults or Au−GFP−INT vaults detached from the beads of three preparations (as described above) were pooled together, and 90 μL samples were placed in a 225 μL quartz cuvette. The sample was illuminated (using a Fluorolog 2, ISA Jobin Yvon- Spex, Edison, NJ) at 468 nm until the emission at 511 nm was stable. One microliter of 10 μM congo red in PBS was added and thoroughly mixed, and the fluorescence emission at 511 nm was recorded over time (after the ~10 s delay due to sample addition and mixing). For comparison, soluble GFP−INT or Au−GFP−INT was diluted until the GFP emission intensity at 511 nm was approximately equal to that of vault-containing samples and assayed similarly. Fluorescence intensity as a function of time was fit to a three-parameter exponential decay with SigmaPlot 2000 (v6.00). The decay time was calculated as the time at which the fluorescence was quenched to 1% of its initial intensity.

6-His-GFP incorporated onto the Au−mINT complex was encapsulated in vaults and purified as described above. GFP−Au−INT vaults detached from the antibody−agarose beads of two preparations were pooled together, and 80 μL samples were placed in a 225 μL quartz cuvette. Samples were excited at 468 nm, and the emission spectra (average of three scans) were recorded from 490 to 600 nm. Free His-GFP (with and without gold) in PBS pH 7.6 was scanned similarly as a quantitative positive control.

Acknowledgment. We thank Hedi Roseboro for infection of Sf9 cells and preparation of infected cell pellets, Daniel Buehler for preparation of recombinant mINT, Wendy Fujioka for assistance with 6-His-GFP western blots, Dr. Cheng Lai for making the GFP−INT pET28 construct, and Mike Lo and Dr. Miguel Garcia-Garibay for use of fluorescence instrumentation. This work was supported by National Science Foundation NIRT Grant MCB-02 10690.

REFERENCES AND NOTES

1. Sparreboom, A.; Barker, S. D.; Verweij, J. Paclitaxel Repackaged in an Albumin-Stabilized Nanoparticle: Handy or Just a Dandy? *J. Clin. Oncol.* **2005**, *23*, 7765–7767.
2. Allen, T. M.; Cullis, P. R. Drug Delivery Systems: Entering the Mainstream. *Science* **2004**, *303*, 1818–1822.
3. Torchilin, V. P.; Lukyanov, A. N. Peptide and Protein Drug Delivery to and into Tumors: Challenges and Solutions. *Drug Discovery Today* **2003**, *8*, 259–266.
4. Jin, S.; Ye, K. Nanoparticle-Mediated Drug Delivery and Gene Therapy. *Biotechnol. Prog.* **2007**, *23*, 32–41.
5. Noad, R.; Roy, P. Virus-like Particles as Immunogens. *Trends Microbiol.* **2003**, *11*, 438–444.
6. Garcea, R. L.; Gissmann, L. Virus-like Particles as Vaccines and Vessels for the Delivery of Small Molecules. *Curr. Opin. Biotechnol.* **2004**, *15*, 513–517.
7. Mastrobattista, E.; van der Aa, M. A. E. M.; Hennink, W. E.; Crommelin, D. J. A. Artificial Viruses: A Nanotechnological Approach to Gene Delivery. *Nat. Rev. Drug Discovery* **2006**, *5*, 115–121.
8. Sharma, A.; Sharma, U. Liposomes in Drug Delivery: Progress and Limitations. *Int. J. Pharm.* **1997**, *154*, 123–140.
9. Andresen, T. L.; Jensen, S. S.; Jorgensen, K. Advanced Strategies in Liposomal Cancer Therapy: Problems and Prospects of Active and Tumor Specific Drug Release. *Prog. Lipid Res.* **2005**, *44*, 68–97.
10. Allen, C.; Maysinger, D.; Eisenberg, A. Nano-Engineering Block Copolymer Aggregates for Drug Delivery. *Colloids Surf., B* **1999**, *16*, 3–27.
11. Hatefi, A.; Amsden, B. Biodegradable Injectable *In Situ* Forming Drug Delivery Systems. *J. Controlled Release* **2002**, *80*, 9–28.
12. Mikyas, Y.; Makabi, M.; Raval-Fernandes, S.; Harrington, L.; Kickhoefer, V. A.; Rome, L. H.; Stewart, P. L. Cryoelectron Microscopy Imaging of Recombinant and Tissue Derived Vaults: Localization of the MVP N-Termini and VPARP. *J. Mol. Biol.* **2004**, *344*, 91–105.
13. Kong, L. B.; Siva, A. C.; Rome, L. H.; Stewart, P. L. Structure of the Vault, a Ubiquitous Cellular Component. *Structure* **1999**, *7*, 371–379.
14. Kedersha, N. L.; Miquel, M.-C.; Bittner, D.; Rome, L. H. Vaults. II. Ribonucleoprotein Structures Are Highly Conserved among Higher and Lower Eukaryotes. *J. Cell Biol.* **1990**, *110*, 895–901.
15. Kickhoefer, V. A.; Rajavel, K. S.; Scheffer, G. L.; Dalton, W. S.; Scheper, R. J.; Rome, L. H. Vaults Are Up-Regulated in Multidrug-Resistant Cancer Cell Lines. *J. Biol. Chem.* **1998**, *273*, 8971–8974.
16. Siva, A. C.; Raval-Fernandes, S.; Stephen, A. G.; Femina, M. J. L.; Scheper, R. J.; Kickhoefer, V. A.; Rome, L. H. Up-Regulation of Vaults May Be Necessary but Not Sufficient for Multidrug Resistance. *Int. J. Cancer* **2001**, *92*, 195–202.
17. Scheffer, G. L.; Wijngaard, P. L. J.; Flens, M. J.; Izquierdo, M. A.; Slovak, M. L.; Pinedo, H. M.; Meijer, C. J. L. M.; Clevers, H. C.; Scheper, R. J. The Drug Resistance-Related Protein LRP is the Human Major Vault Protein. *Nat. Med.* **1995**, *1*, 578–582.
18. Berger, W.; Steiner, E.; Grusch, M.; Elbling, L.; Micksche, M. Vaults and the Major Vault Protein: Novel Roles in Signal Pathway Regulation and Immunity. *Cell. Mol. Life Sci.* **2009**, *66*, 43–61.
19. Kowalsk, M. P.; Dubouix-Bourandy, A.; Bajmoczi, M.; Golan, D. E.; Zaidi, T.; Coutinho-Sledge, Y. S.; Gygi, M. P.; Gygi, P. S.; Weimer, E. A. C.; Pier, G. B. Host Resistance to Lung Infection Mediated by Major Vault Protein in Epithelial Cells. *Science* **2007**, *317*, 130–132.
20. Anderson, D. H.; Kickhoefer, V. A.; Sievers, S. A.; Rome, L. H.; Eisenberg, D. Draft Crystal Structure of the Vault Shell at 9 Å Resolution. *PLoS Biol.* **2007**, *5*, 2661–2670.
21. Tanaka, H.; Kato, K.; Yamashita, E.; Sumizawa, T.; Zhou, Y.; Yao, M.; Iwasaki, K.; Yoshimura, M.; Tsukihara, T. The Structure of Rat Liver Vault at 3.5 Angstrom Resolution. *Science* **2009**, *323*, 384–388.
22. Kedersha, N. L.; Heuser, J. E.; Chugani, D. C.; Rome, L. H., III. Vault Ribonucleoprotein Particles Open into Flower-like Structures with Octagonal Symmetry. *J. Cell Biol.* **1991**, *112*, 225–235.
23. Kong, L. B.; Siva, A. C.; Kickhoefer, V. A.; Rome, L. H.; Stewart, P. L. RNA Location and Modeling of a WD40 Repeat Domain within the Vault. *RNA* **2000**, *6*, 890–900.

24. Stephen, A. G.; Raval-Fernandes, S.; Huynh, T.; Torres, M.; Kickhoefer, V. A.; Rome, L. H. Assembly of Vault-like Particles in Insect Cells Expressing Only the Major Vault Protein. *J. Biol. Chem.* **2001**, *276*, 23217–23220.
25. Kickhoefer, V. A.; Garcia, Y.; Mikyas, Y.; Johansson, E.; Zhou, J. C.; Raval-Fernandes, S.; Minoofar, P.; Zink, J. I.; Dunn, B.; Stewart, P. L.; Rome, L. H. Engineering of Vault Nanocapsules with Enzymatic and Fluorescent Properties. *Proc. Natl. Acad. Sci. U.S.A.* **2005**, *102*, 4348–4352.
26. Kickhoefer, V. A.; Han, M.; Raval-Fernandes, S.; Poderycki, M. J.; Moniz, R. J.; Vaccari, D.; Silvestry, M.; Stewart, P. L.; Kelly, K. A.; Rome, L. H. Targeting Vault Nanoparticles to Specific Cell Surface Receptors. *ACS Nano* **2009**, *3*, 27–36.
27. Goldsmith, L. E.; Yu, M.; Rome, L. H.; Monbouquette, H. G. Vault Nanocapsule Dissociation into Halves Triggered at Low pH. *Biochemistry* **2007**, *46*, 2865–2875.
28. Poderycki, M. J.; Kickhoefer, V. A.; Kaddis, C. S.; Raval-Fernandes, S.; Loo, J. A.; Rome, L. H. The Vault Exterior Shell Is a Dynamic Structure That Allows Incorporation of Vault-Associated Proteins into Its Interior. *Biochemistry* **2006**, *45*, 12184–12193.
29. Ng, B. C.; Yu, M.; Ajaykumar, G.; Rome, L. H.; Monbouquette, H. G.; Tolbert, S. H. Encapsulation of Semiconducting Polymers in Vault Protein Cages. *Nano Lett.* **2008**, *8*, 3503–3509.
30. Yu, M.; Ng, B. C.; Rome, L. H.; Tolbert, S. H.; Monbouquette, H. G. Reversible pH Lability of Cross-Linked Vault Nanocapsules. *Nano Lett.* **2008**, *8*, 3510–3515.
31. Kickhoefer, V. A.; Siva, A. C.; Kedersha, N. L.; Inman, E. M.; Ruland, C.; Streuli, M.; Rome, L. H. The 193-kD Vault Protein, VPARP, is a Novel Poly(ADP-Ribose) Polymerase. *J. Cell Biol.* **1999**, *146*, 917–928.
32. van Zon, A.; Mossink, M. H.; Schoester, M.; Scheffer, G. L.; Scheper, R. J.; Sonneveld, P.; Wiemer, E. A. C. Structural Domains of Vault Proteins: A Role for the Coiled Coil Domain in Vault Assembly. *Biochem. Biophys. Res. Commun.* **2002**, *291*, 535–541.
33. Hainfeld, J. F.; Powell, R. D. New Frontiers in Gold Labeling. *J. Histochem. Cytochem.* **2000**, *48*, 471–480.
34. Hainfeld, J. F.; Liu, W.; Halsey, C. M. R.; Freimuth, P.; Powell, R. D. Ni−NTA−Gold Clusters Rarget His-Tagged Proteins. *J. Struct. Biol.* **1999**, *127*, 185–198.
35. Richmond, T. A.; Takahashi, T. T.; Shimkhada, R.; Bernsdorf, J. Engineered Metal Binding Sites on Green Fluorescence Protein. *Biochem. Biophys. Res. Commun.* **2000**, *268*, 462–465.
36. Schmitt, J.; Hess, H.; Stunnenberg, H. G. Affinity Purification of Histidine-Tagged Proteins. *Mol. Biol. Rep.* **1993**, *18*, 223–230.
37. Nanoprobes, Detection of Nanogold-Labeled Molecules on Gels http://www.nanoprobes.com/App1A.html, Yaphank, NY, 1998.